Proceedings of the Fifth IASTED International Conference
BIOMEDICAL ENGINEERING
February 14–16, 2007, Innsbruck, Austria
ISBN Hardcopy: 978-0-88986-648-5 / CD: 978-0-88986-649-2

TOWARDS A LOW-COST OPTICAL BIOSENSOR SYSTEM FOR BIOMEDICAL IMMUNOASSAY APPLICATIONS

J. W. Gardner[1], A. Apostolidou[1], M. Cole[1], C. Dowson[2], S. Edmunds[3], and G. Sehra[1]

[1]School of Engineering and [2]Department of Biological Sciences
University of Warwick, Coventry, CV4 7AL, UK
[3]Agrisol Ltd, 49 High Street, Ashcott, Somerset, TA7 9QA, UK
Email: j.w.gardner@warwick.ac.uk

ABSTRACT

A novel, low-cost optical measurement system has been designed for biomedical applications such as immunoassays. The system comprises a rapid-prototyped ABS plastic housing, 500 nm LED source, 530 nm UV filter, and 540 nm silicon photodiode receiver with a custom-built high gain precision amplifier. The sensor system has been designed to measure the fluorescence of different bioliquids in a standard glass test-tube. In addition, a small disc magnet can be inserted to enhanced signal-to-noise in liquids containing fluorophore-labelled magnetic beads. Our preliminary results show that the baseline optical signal depends weakly on the refractive index of the liquid and more strongly on its opaqueness. Removing this baseline signal permits the measurement of FTIC solutions down to concentrations of about 100 nMol. In addition, the insertion of the magnet was found to enhance significantly the optical signal in translucent liquids with low bead concentrations but, interesting, not in opaque ones. We believe that this low-cost (less than €150) optical immunoassay sensor has potential applications such as detecting progesterone and bacteria levels in milk, water, saliva, urine, and blood.

KEY WORDS

Medical devices, biosensors, immunoassay, optical system.

1. Introduction

Biosensors are basically devices that sense biological molecules, such as enzymes, antibodies, receptors and nucleic acids by exploiting a specific molecular recognition system [1]. These biomolecules could be part of a cell, organelle or tissue but are usually extracted and immobilised onto a test surface. The specific binding of the target biomolecule (e.g. antibody) to a molecule immobilised at the surface (e.g. an antigen) with a fluorescent label is known as optical immunoassay. Figure 1(a) illustrates the principle of fluorescence used in such an optical biosensor. An external light source (e.g. laser) is used to illuminate a fluorescent molecule and thus stimulate a transition from the stable ground energy state S_0 to a higher energy state which relaxes down to a lower excited state S_1 by a non-radiative process. Fluorescence occurs when the molecule relaxes further to the ground state and emits a photon of lower energy (−hν) than that of the original light source. The fluorescent light is then collected by a receiver (e.g. photomultiplier tube). A competing process is also shown in Figure 1(a) called phosphorescence in which molecules relax radiationless via an energy state T_0. However this is, generally, a less probable and slower process with lower energies; so should not cause too much interference.

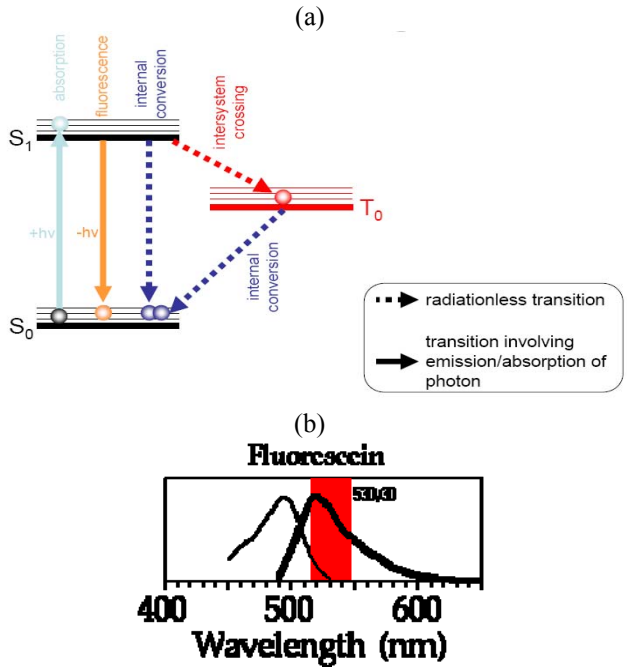

Fig. 1: (a) Principle of fluorescence illustrated by the Jablonski energy level diagram, (b) spectra of typical source and fluorescein UV emission (peak 530 nm).

Our study here uses the most common type of fluorescent marker dye called fluorescein that can be conjugated to proteins via primary amines, i.e. lysines. Figure 1(b) shows its excitation spectrum (thin solid line) – normally

by a 488 nm argon laser – and resulting emission spectrum (thick line) of fluorescein. The shaded area shows the wavelength band (515 to 545 nm) of an optical filter commonly used to measure the fluorescence. Unfortunately, part of the emitted light will pass through the filter and create an interfering signal. The intensity of the light source is typically many of orders of magnitude higher than that of the fluorescent source and so this can pose a significant problem.

Optical immunoassay sensors have been developed for a number of different applications. For example, one research group has used it to identify *pseudomonas* strains in milk, water and cheeses [2]. A second research group has used it to detect progesterone levels in milk [3] which is important in the profiling of the oestrus levels in diary cattle. Here we are interested in the detection of progesterone and bacteria levels in milk and have previously reported measurements employing a non-specific SAW- based acoustic method [4,5].

In this paper we report upon the design, fabrication and testing of a novel optical biosensor system for immunoassay applications. Our ultimate objective is to make a low-cost (< €150), portable device that employs low-cost light-emitting diodes and photodiodes rather than expensive argon lasers and photomultipliers. The challenge here is to design a simple biological sample preparation method and to extract the relatively low fluorescent signals derived from the biomolecules in liquids or immobilised on the surface of magnetic beads known as Dynabeads.

Figure 3 shows how antibody-antigen conjugates can be formed on the surface of a glass test-tube while Figure 4 shows the different commercial magnetic beads available.

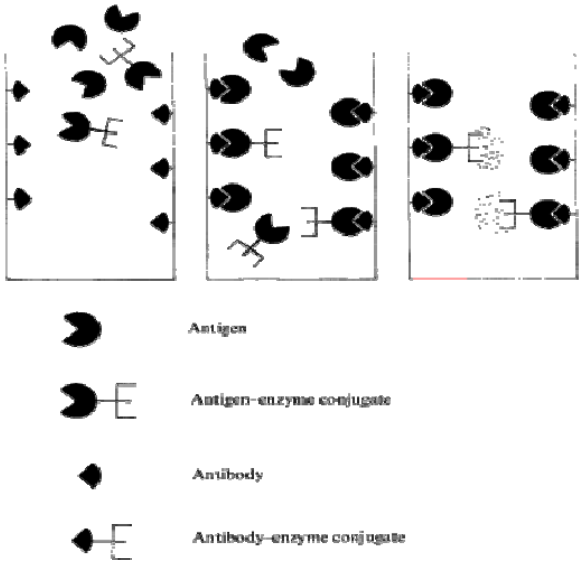

Fig. 2: Basic principle of antibody-antigen conjugation onto a fixed surface.

In our experiments we used commercially-available magnetic beads called Dynabeads that have been labelled with protein G and anti-progesterone monoclonal antibody with FITC label. The beads are magnetic in nature and so will move towards a DC magnet field when they are uniformly dispersed within a liquid. This is an attractive option because the beads not only speed up the binding process but may then be used to enhance the fluorescent signal.

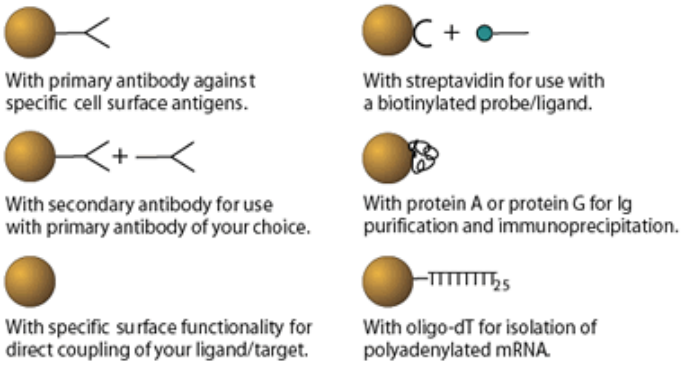

Fig. 3: Different types of Dynabeads commercially available.

2. Optical design and set-up

A schematic of the cross-section of the optical sensing system is shown in Figure 4. The housing (base is about. 50 mm by 67 mm) was designed using commercial 3-D CAD software and manufactured from ABS plastic in about 1 hour using a thermal 3-D rapid prototyping unit (estimated cost €5 per housing). It was then sprayed all over with glossy black paint to stop any light crossing over.

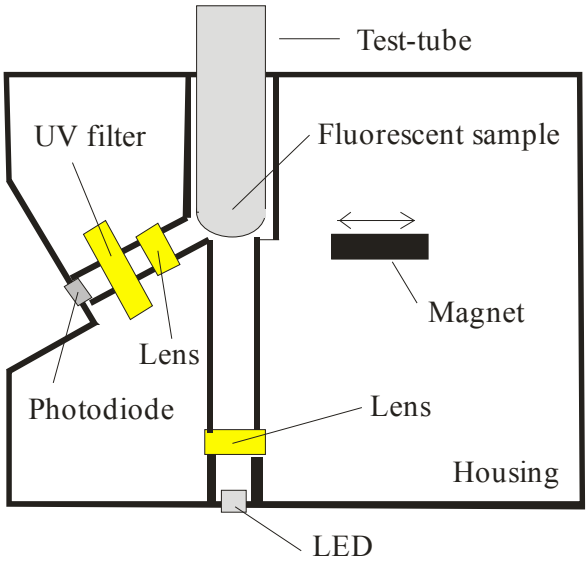

Fig. 4: Schematic cross-section of optical biosensor system (not to exact scale).

A low-cost LED (LXHL-NE98, Luxeon V star, €15) with a Lambertian radiation pattern with 75° half-angle was selected as the light source. Specifically a cyan light source was chosen with a typical peak wavelength of 505 nm (minimum 490 nm) and 30 nm spectral half-width. It was driven at a DC voltage of 6 V to produce a forward current of 200 mA and luminous flux typically of about 50 lumens (maximum permitted is 120 ln). The emitted light is collimated by the plastic housing and can be focused further using a lens (not used here). Cyan light then illuminates the rounded bottom of a Pyrex® glass test-tube containing the fluorescent sample. Some light will be reflected back at the air-glass (*ca*. 4%) and glass-liquid interface (*ca*. 0.4%) thus reducing the amount available for fluorescing. Light reaching the liquid may also be diffusively scattered back, absorbed within the liquid or reach fluorescent sites and stimulate UV radiated light. Part of light coming from the fluorescent biomolecules will again be scattered, absorbed in the liquid, or reflected back at the liquid-glass and glass-air interfaces. The rest of the light will travel in the direction of the photodetector first reaching an optical high pass filter of 530 nm (Glen Spectra Emitter XF32007; permitting the transmission of the desired fluorescent UV light signal at peak of 530 nm. A small lens is used to focus the light onto the small sensing area of a silicon photodiode (Hamamatsu, S6429, €9) with peak sensitivity of 0.27 A/W at a wavelength of 540 nm. An optical model has been developed estimating the geometrical losses, reflection losses, quantum efficiency losses at each stage of the system and indicates that the photocurrent generated by the fluorescent light from FTIC solutions will be very low and in the worst case scenario of the order of a few picoamps [6].

The optical system was assembled and Figure 5 shows a photograph of the sensing unit. A small disc magnet can be slid across and underneath the glass test-tube when using liquids containing magnetic beads.

3. Electronic interface circuitry

The low photocurrents estimated by our optical model necessitate the design of a high-gain low-noise amplifier circuit in order to obtain a reasonable voltage output. Figure 6 shows a schematic of the circuit designed to measure the photocurrents generated by the fluorescent samples. The input operational amplifier U1 is a high-precision DiFET (OPA602) and employed in a trans-impedance circuit configuration. The voltage output V_{O1} of the first stage is governed by a high value feedback resistor R_5 and is simply related to the photogenerated diode current I_{PD} by:

$$V_{O1} = R_5 I_{PD} \qquad (1)$$

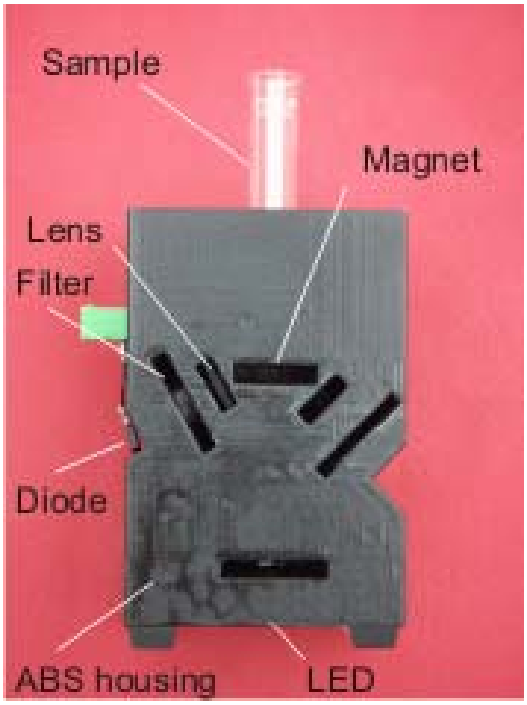

Fig. 5: Photograph of the optical set-up of the biosensor system.

The feedback resistance was set by a precision metal film resistor R5 to a value of 470 MΩ and so a 2 pA photocurrent should produce a one millivolt output.

If necessary, the output from the first stage can be fed into a high pass RC filter circuit (not shown). This could be used when driving the LED with periodic or pulsed signals (f > RC) in order to make transient measurements.

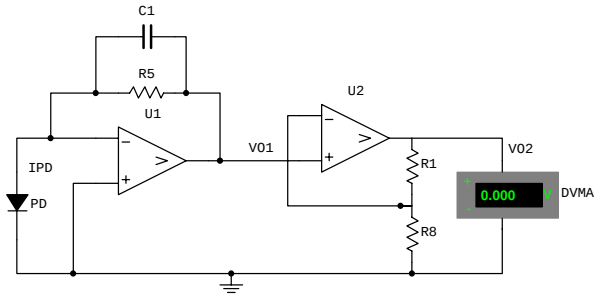

Fig. 6: Schematic diagram of the two-stage amplifier circuit for the photodiode PD (simplified version of final PCB layout).

The final stage is a conventional non-inverting voltage amplifier again using the OPA602 low input bias op-amp (U2) with the gain selectable from a choice of five precision resistors (only resistor R1 shown). The voltage gain *G* of the second stage is given by

$$G = \frac{V_{O2}}{V_{O1}} = \left[1 + \frac{R_{1,2,4-7}}{R_8}\right] \quad (2)$$

R_8 is set to a value of 470 Ω and so the second stage gain is selectable from 10 to 100,000. Consequently, a 2 femtoamp photocurrent should produce a 100 mV output voltage V_{O2}. The output voltage is related to the photocurrent (which in turn can be related back to the fluorescent light signal) and given by

$$V_{O2} = \left[1 + \frac{R_{1,2,4-7}}{R_8}\right] R_5 I_{PD} \quad (3)$$

The output voltage connected fed via a standard BNC co-axial cable to either a digital storage oscilloscope or a precision digital voltmeter (DVMA) capable of measuring down to microvolts.

Figure 7 shows a photograph of the optical amplifier circuit hardwired on to a printed-circuit board and housed within an earthed metal case.

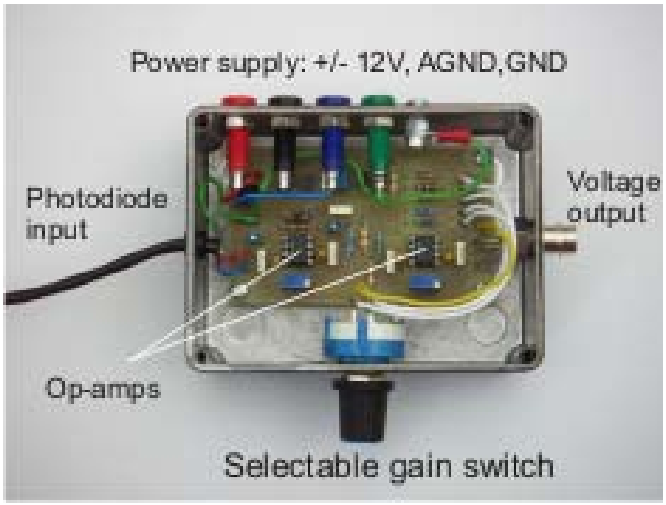

Fig. 7: Photograph of amplifier circuitry.

4. Experimental results

0.0078 g of FITC dust was weighed out and diluted in 20 ml of buffer solution; the buffer solution was initially Tris/HCl with a pH of 8. Then 2 ml of the FITC solution was added to 18 ml of buffer in order to dilute the concentration by a factor of 10. The procedure was repeated 6 more times to create a set of seven molarities from 1 mmol to 1 nmol solutions. The fluorescence of these samples also was tested in a commercial fluorometer (E&G 1420 Victor Multilabel counter) for benchmarking.

Figure 8 shows the variation of the photocurrent with the different molarities of the FTIC solutions. The solid line is the excellent fit to the experimental data by a 5-parameter sigmoid function. This plot shows that there is a significant background light signal giving rise to a baseline photocurrent of *ca*. 0.7 nA and a saturation current of 2.1 nA. The saturation effect is associated with the light signal and not the circuitry itself that shows saturation at high gains of 2.5 nA. We can also see that the circuit with a second stage gain of just 10 measures molarities at and above 1,000 nmol.

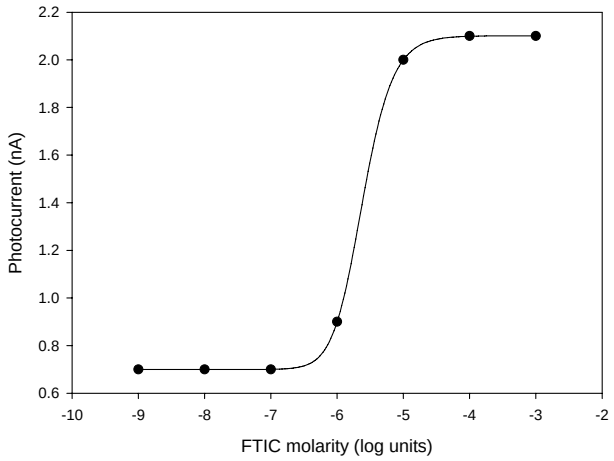

Fig. 8: Variation of photodiode current with molarity of the FTIC solution.

A set of experiments were carried out using water, Tris/HCl (pH 8), skimmed, semi-skimmed and full fat milk with and without different concentrations of protein G coated Dynabeads. The concentration of the beads was increased linearly be simply adding drops to a standard 20 ml sample.

The different milk samples showed no variation in light signal with different fat contents (0, 2 and 4%) and interestingly also showed no increase when the magnet was applied. This suggests that the milk limits the visibility of beads by producing considerable scattering of sites.

Milk (4% fat) was found to exhibit the highest background sensor value of 10.9±0.1 V, while that for water was much lower at 6.5±0.1 V, and Tris/HCl slightly lower than water at 6.2±0.1 V.

From these initial observations, we could see that there is a small affect of the refraction index/pH of the liquid on the sensor output voltage. Milk gave a very high background voltage of 10.8 V that could not be explained by a difference in refractive index alone. This suggests that a considerable amount of the background signal is associated with light scattering back into the detector from an opaque solution.

Table 1 shows the affect of the protein G bead concentration in water on the sensor output voltage. Values are given for before and after the magnet have been applied attracting beads to the bottom of the glass test-tube. The concentration of beads per ml in the solutions containing the drops has been estimated to be approximately 10^9 beads per ml per drop.

Table 1: Effect of the number of drops of protein G in water on the output voltage of the photodiode circuit before and after magnet is introduced.

No of drops of protein G in H_2O	Voltage (V) before using magnet	Voltage (V) after using the magnet
0	6.308	6.308
3	8.247	8.985
5	8.946	9.472
7	9.517	9.987
10	10.404	10.756
13	10.854	11.005

Figures 9 show plots of the output sensor voltages for the different concentrations of fluorescent beads - before and after the magnet has been applied. The output voltage clearly increases with bead concentration, as expected, but the influence of the magnet decreases with increasing concentration of beads. This effect is shown more clearly in Figure 10 below.

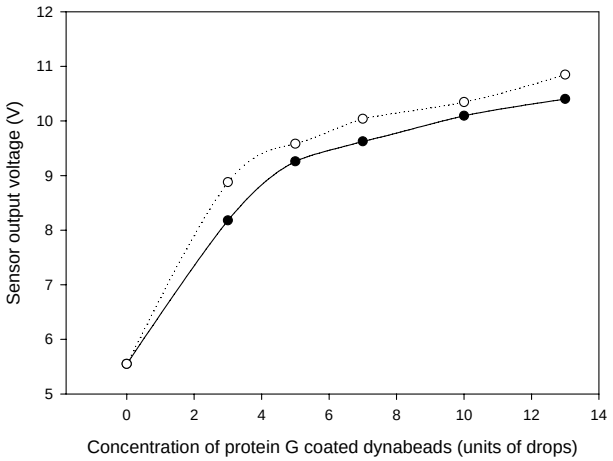

Fig. 9: Sensor output voltage with concentration of fluorescent beads in water (units of drops) before magnet is applied (solid circles) and after application (open circles).

Figure 10 shows the data in Figure 9 reduced to the difference in sensor output voltage before and after the magnet has been applied. This experiment was repeated for solutions of Tris/HCl instead of water and both sets of results have been plotted in Figure 10. It is evident that signal enhancement is highest for the lowest concentration of beads and that the effect is, within experimental data, the same for both water and Tris/HCl buffer solutions. This differential response can be used to remove most of the background signal and help predict underlying fluorescence levels associated with reactions.

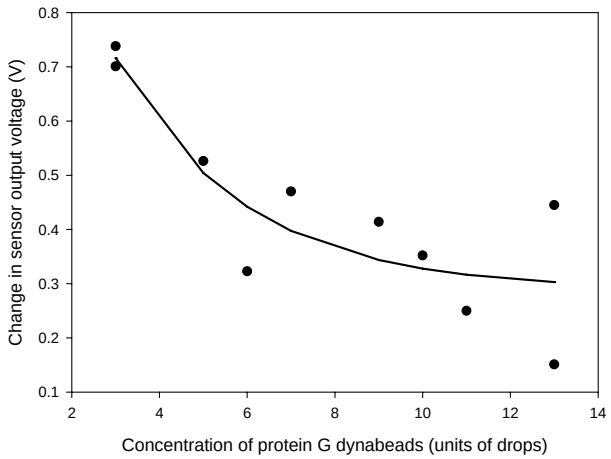

Fig. 10: Change in sensor output voltage when magnet is applied against the concentration of G protein beads in water and Tris/HCl samples (units of drops).

However, our results with milk suggest that the magnetic enhancement might not work well with opaque samples like blood as opposed to translucent samples such as urine or saliva.

5. Conclusion

We have designed and built a prototype optical biosensor system that can be used for different immunoassay applications (see Figure 11).

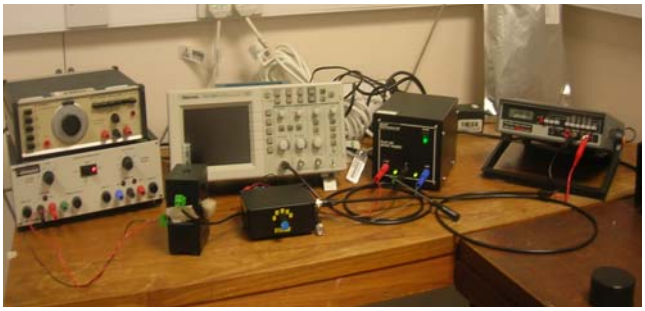

Fig. 11: Prototype optical biosensor system for immunoassay application showing DC LED power supply, digital scope, circuit DC supply (±12 V), and DVM (from left to right).

Significant background light signals were detected by the photodiode and corresponded to the nanoamp level rather

than the picoamps level predicted by our basic theory. This suggests that there is significant scattering of light back from the liquid itself which was not accounted for in our model.

Moreover, this background light signal was observed to relate to the nature of the liquid being tested and weakly related to its refractive index. This is expected because the light transmission and reflection coefficients depend upon the refractive indexes of the liquid at the glass-liquid interface.

It is important that this background light signal is removed and this can be achieved by offsetting the voltage in order to achieve higher sensitivities. It has been estimated that the sensitivity of the unit is currently 1,000 nmol of FTIC but can be used to less than 100 nmol through voltage offset circuitry.

We have shown that our low-cost optical sensor system will not only detect different concentrations of FTIC solutions but also detect different concentrations of G protein coated dynabeads. The sensor output has been found, as expected, to increase significantly with the concentration of beads in water and Tris/HCl buffers solutions. In the case of transparent solutions, the application of a magnet was found to enhance the light signal and with the differential signal being greatest (and hence sensitivity) as the lowest bead concentration observed.

It is relatively straightforward in manufacturing terms to reduce both the size of the plastic housing and the electronic circuitry (through surface mount components). Moreover the components can be integrated into a simple, portable optical instrument. The cost to manufacture such an instrument is estimated to be about €150.

Finally, we believe that this system can be used to measure progesterone and bacterial levels in water, milk and possibly urine, saliva and blood. However, the use of magnetic beads to enhance sensitivity may be restricted to translucent liquids. Future work is being directed towards these applications and could offer a low-cost portable immunoassay system.

Acknowledgement

We wish to thank Dr. Peter Kimber (Warwick University) for his help in the design and fabrication of the ABS plastic housing.

References

[1] J.W. Gardner, Microsensors, 1994, John Wiley & Sons Ltd, Chichester, 320pp.

[2] F. Lerichea *et al*., Alteration of raw milk cheese by pseudomonas ssp.: monitoring the sources of contamination using fluorescent spectroscopy and metabolic profiling, *Journal of Microbiological Methods, 59, 2004, 33-41.*

[3] R. Mehmet et al., Using milk progesterone assay at the time of oestrus and post-mating for diagnosing early pregnancy in Anatolian water buffalo, *Turkish Vetinarian Animal Science, 28, 2004, 513-518.*

[4] G. Sehra, M. Cole M, and J.W. Gardner, Miniature tasting system based on dual SH-SAW sensor device: an electronic tongue, *Sensors and Actuators B, 103, 2004, 233-239.*

[5] J.W. Gardner, M. Cole, C.G. Dowson, P. Newton and G. Sehra, Smart acoustic sensor for the detection of bacteria in milk, *IASTED International Conference on Biomedical Engineering*, Innsbruck, Austria, 16-18 Feb 2005.

[6] A. Apostolidou, Building an optical biosensor system for immunoassay applications, *2006, MSc thesis, University of Warwick, Coventry, UK*.